

Mechanics of Streptavidin-Coated Giant Lipid Bilayer Vesicles: A Micropipet Study

Pasut Ratanabanangkoon,[†] Michael Gropper,[‡] Rudolf Merkel,[§]
Erich Sackmann,[‡] and Alice P. Gast*

Department of Chemical Engineering, Stanford University, Stanford, California 94305-5025,
Department of Biophysics-E22, Technical University of Munich, D-85748 Garching, Germany,
Forschungszentrum Jülich, Institut für Schichten und Grenzflächen (ISG-4),
D-52425 Jülich, Germany, and Department of Chemical Engineering,
Massachusetts Institute of Technology, Cambridge, Massachusetts 02139

Received July 17, 2002. In Final Form: November 4, 2002

To understand the effects of a crystalline protein layer on bilayer properties, we studied the mechanical properties of avidin- and streptavidin-coated giant lipid bilayer vesicles. The giant vesicles (20–60 μm) are made from a mixture of SOPC and biotinylated phospholipids via electroformation. Using micropipet manipulation, we showed that the presence of a monomolecular layer of noncrystalline avidin on the vesicle surface increases the membrane bending rigidity but does not significantly alter the elastic area expansion modulus of the vesicle. When the vesicles were coated with streptavidin, the protein crystallizes on the bilayer surface, resulting in a rigid polycrystalline membrane. These vesicles display unique roughened spherical or prolate ellipsoidal shapes, depending on the differences in crystal morphologies. Upon aspiration with micropipets, the vesicles first showed rapid permanent deformation at low strain, followed by a slower viscoelastic response above a certain threshold. Despite their extremely rigid appearance, the existence of a polycrystalline shell does not increase the toughness of streptavidin-coated vesicles above that of uncoated vesicles. The origin of these properties can be traced to the unique ligand–receptor interactions between streptavidin and biotinylated phospholipids in the bilayer membrane. The findings offer greater understandings of complex phenomena involving crystalline protein layers on the surface of cell membranes, in addition to providing information for the development of various applications involving the immobilization of functionalized molecules on lipid bilayer substrates.

Introduction

Properties of lipid bilayer membranes and membrane–protein complexes have been of great interest and the subject of numerous studies due to their physical and biological importance and potential applications.^{1–3} In particular, they serve as simplified models to the complex and inhomogeneous properties of actual cell membranes. The possibility of incorporating molecules into the membrane to systematically alter its composition allows the separate study of individual membrane components and has led to significant understanding of a number of membrane properties and cellular functions.^{4–8} The ability to vary bilayer composition also allows custom tailoring of bilayer surfaces to suit various applications, such as

the attachment of biomolecules to inorganic surfaces. Through Langmuir–Blodgett^{9,10} or vesicle fusion^{11–13} techniques, lipid bilayers are used to create fluid layers on solid–liquid interfaces for the attachment of other functionalized molecules.^{1,14} Functionalization of the bilayer surface often involves the binding of an intermediate monomolecular layer of protein which itself acts as either a receptor or a support for the attachment of other ligands and biomolecules. In some biosensor applications, the formation of ordered arrays of functionalized molecules on supported bilayers is desired. This can be achieved by crystallizing an underlying protein layer into an ordered array. While it is clear that certain alterations made to the bilayer membrane can affect its properties and thus its uses, the change in the bilayer properties due to the presence of an outer crystalline protein layer has not been thoroughly investigated.

Through the use of giant vesicles as model bilayers, we studied the effect of a surface crystalline protein layer on the mechanical properties of the membrane. In particular, we used micropipet aspiration to probe the membrane responses and material properties of vesicles that exhibited (a) no coating, (b) a crystalline streptavidin layer at the surface, or (c) a monolayer of homogeneous yet noncrystallizable protein avidin.

* To whom correspondence may be addressed at the Massachusetts Institute of Technology. Phone: (617) 253-1403. FAX: (617)-253-8388. E-mail: gast@mit.edu.

[†] Stanford University. E-mail: pasut@leland.stanford.edu.

[‡] Technical University of Munich. E-mail: Michael Gropper, michael.gropper@web.de; Rudolf Merkel, r.merkel@fz-juelich.de.

[§] Institut für Schichten und Grenzflächen. E-mail: r.merkel@fz-juelich.de.

(1) Sackmann, E. *Science* **1996**, *271*, 43–48.

(2) Luisi, P. L.; Walde, P. *Giant Vesicles*; John Wiley & Sons, Ltd: New York, 2000; Vol. 6.

(3) Cevc, G. *Phospholipids handbook*; Marcel Dekker: New York, 1993.

(4) Dietrich, C.; Yang, B.; Fujiwara, T.; Kusumi, A.; Jacobson, K. *Biophys. J.* **2002**, *82*, 274–284.

(5) Hackl, W.; Barmann, M.; Sackmann, E. *Phys. Rev. Lett.* **1998**, *80*, 1786–1789.

(6) Schindler, M.; Osborn, M. J.; Koppel, D. E. *Nature* **1980**, *283*, 346–350.

(7) Parlati, F.; McNew, J. A.; Fukuda, R.; Miller, R.; Sollner, T. H.; Rothman, J. E. *Nature* **2000**, *407*, 194–198.

(8) Needham, D.; Macintosh, T. J.; Lasic, D. D. *Biochim. Biophys. Acta* **1992**, *1108*, 40–48.

(9) Blodgett, K. B. *J. Am. Chem. Soc.* **1935**, *57*, 1007.

(10) Langmuir, I. *Trans. Far. Soc.* **1920**, *15*, 62.

(11) Kalb, E.; Frey, S.; Tamm, L. K. *Biochim. Biophys. Acta* **1992**, *1103*, 307–316.

(12) Tamm, L. K.; McConnell, H. M. *Biophys. J.* **1985**, *47*, 105–113.

(13) Brian, A. A.; McConnell, H. M. *Proc. Natl. Acad. Sci. U.S.A.* **1984**, *81*, 6159–6163.

(14) Zasadzinski, J. A.; Viswanathan, R.; Madsen, L.; Garnæs, J.; Schwartz, D. K. *Science* **1994**, *263*, 1726–1733.

Streptavidin, a tetrameric globular protein that has an unusually high binding affinity (10^{-15} M)¹⁵ for biotin, is commonly used as a linker to immobilize various biotinylated molecules to surfaces. Streptavidin can crystallize into highly ordered arrays on various two-dimensional (2D) surface such as lipid monolayers,^{16–23} lipid bilayers at the solid–liquid interface,²⁴ lipid nanotubes,^{25,26} and, recently, giant bilayer vesicles.²⁷ The presence of two pairs of biotin-binding sites on opposing sides of each streptavidin molecule, along with its high affinity for biotin, results in extensive use as a molecular linker in various applications.^{28–30}

This work aims toward a fundamental understanding of self-assembly processes in biological systems. It has been known that hundreds of species of bacteria and archaea found in various environments contain a crystalline layer of surface proteins at the cell surface called s-layers. Specific functions of s-layer proteins vary with different bacterial species and include nutrient transport, adhesion sites, and protective functions, especially in archaea lacking a rigid wall layer.^{31,32} These proteins self-assemble onto cell surfaces via noncovalent forces such as electrostatic and hydrophobic interactions. In this study the streptavidin–biotin receptor–ligand interaction system can also be made to produce crystalline layers imparting some mechanical strength to the bilayer. Attempts to study the properties of the natural crystalline layer on actual cells are often complicated by other underlying structural components such as peptidoglycan layers in addition to the complex cytoplasmic composition and the minute size of bacteria. Crystallizing proteins on giant bilayer vesicles provides us with a similar, well-defined system that is easy to study and manipulate. The unique properties of these structures greatly facilitate both a fundamental understanding of molecular self-assembly and protein–membrane interactions and potential applications involving the immobilization of functionalized molecules on bilayer membranes.

(15) Bayer, E. A.; Benhur, H.; Wilchek, M. *Methods Enzymol.* **1990**, *184*, 80–89.

(16) Darst, S. A.; Ahlers, M.; Meller, P. H.; Kubalek, E. W.; Blankenburg, R.; Ribl, H. O.; Ringsdorf, H.; Kornberg, R. D. *Biophys. J.* **1991**, *59*, 387–396.

(17) Frey, W.; Schief, W. R.; Pack, D. W.; Chen, C. T.; Chilkoti, A.; Stayton, P.; Vogel, V.; Arnold, F. H. *Proc. Natl. Acad. Sci. U.S.A.* **1996**, *93*, 4937–4941.

(18) Hemming, S. A.; Bochkarev, A.; Darst, S. A.; Kornberg, R. D.; Ala, P.; Yang, D. S. C.; Edwards, A. M. *J. Mol. Biol.* **1995**, *246*, 308–316.

(19) Ku, A. C.; Darst, S. A.; Kornberg, R. D.; Robertson, C. R.; Gast, A. P. *Langmuir* **1992**, *8*, 2357–2360.

(20) Wang, S.-W.; Poglitsch, C. L.; Yacilla, M. T.; Robertson, C. R.; Gast, A. P. *Langmuir* **1997**, *13*, 5794–5798.

(21) Wang, S.-W.; Robertson, C. R.; Gast, A. P. *Langmuir* **1999**, *15*, 1541–1548.

(22) Scheuring, S.; Müller, D. J.; Ringler, P.; Heymann, J. B.; Engel, A. *J. Microsc.* **1999**, *193*, 28–35.

(23) Farah, S. J.; Wang, S. W.; Chang, W. H.; Robertson, C. R.; Gast, A. P. *Langmuir* **2001**, *17*, 5731–5735.

(24) Calvert, T. L.; Leckband, D. *Langmuir* **1997**, *13*, 6737–6745.

(25) Wilson-Kubalek, E. M.; Brown, R. E.; Celia, H.; Milligan, R. A. *Proc. Natl. Acad. Sci. U.S.A.* **1998**, *95*, 8040–8045.

(26) Ringler, P.; Müller, W.; Ringsdorf, H.; Brisson, A. *Chem. Eur. J.* **1997**, *3*, 620–625.

(27) Ratanabangkoorn, P.; Gropper, M.; Merkel, R.; Sackmann, E.; Gast, A. P. *Langmuir* **2002**, *18*, 4270–4276.

(28) McLean, M. A.; Stayton, P. S.; Sligar, S. G. *Anal. Chem.* **1993**, *65*, 2676–2678.

(29) Koppenol, S.; Stayton, P. S. *J. Pharm. Sci.* **1997**, *86*, 1204–1209.

(30) Samuelson, L. A.; Wiley, B.; Kaplan, D. L.; Sengupta, S.; Kamath, M.; Lim, J. O.; Cazeca, M.; Kumar, J.; Marx, K. A.; Tripathy, S. K. *J. Int. Mater. Syst. Struct.* **1994**, *5*, 305–310.

(31) Sleytr, U. B.; Messner, P.; Pum, D.; Sára, M. *Crystalline bacterial cell surface proteins*; Academic Press: Austin, TX, 1996.

(32) Sleytr, U. B.; Messner, P.; Pum, D.; Sára, M. *Crystalline bacterial cell surface layers*; Springer-Verlag: Berlin, Germany, 1988.

Material and Methods

Preparation of Vesicles. Giant unilamellar vesicles (GUVs) were made by electroformation.³³ The lipids SOPC (1-stearoyl-2-oleoyl-*sn*-glycero-3-phosphocholine) from Avanti Polar Lipids (Alabaster, AL) and biotin-X-DHPE (*N*-((6-(biotinoyl)amino)hexanoyl)-1,2-dihexadecanoyl-*sn*-glycero-3-phosphoethanolamine, triethylammonium salt) from Molecular Probes (Eugene, OR) were mixed in a weight ratio of 10:1 and dissolved in chloroform (DAB9 grade, Sigma-Aldrich Chemie, Deisenhofen, Germany) to a total concentration of 1 mg/mL. Solutions were kept at -70 °C until use. Approximately 50 μ L of this solution were spread on two indium tin oxide coated glass plates, which measured 6 cm \times 6 cm \times 0.1 cm. Lipid-coated glass plates were dried in a vacuum chamber for at least 2 h to remove the solvent. Subsequently, the glass plates were placed in a swelling chamber with the coated sides facing each other. Both plates were held at a distance of 0.5 mm by a thin Teflon spacer. The vesicles were swollen in 2 mL of a 610 mOsm sucrose solution. After filling the chamber, a sinusoidal AC voltage of 1 V amplitude and 10 Hz frequency was applied for 2 h at room temperature. This procedure has a high yield of GUVs of radii between 10 and 60 μ m.

Protein Labeling. Streptavidin and Avidin were purchased from Prozyme Inc. (San Leandro, CA). A portion of each protein was labeled with Texas Red succinimidyl ester (single isomer) (Molecular Probes, Eugene, OR) according to the supplied protocol, with minor modifications. Briefly, the proteins were dissolved in 100 mM sodium bicarbonate buffer, pH 8.3, to a concentration of 2 mg/mL. The fluorescent dye was then dissolved in reagent grade DMSO (Sigma, St. Louis, MO) to a concentration of 10 mg/mL and added to the protein solution according to the desired labeling ratio. The mixture was stirred in the dark at room temperature for 2 h. The labeled protein was separated from the unreacted dye by passing through a size exclusion column packed with Sephadex G25 (Sigma, St. Louis, MO) and eluted with 50 mM sodium phosphate, pH 7.0. The Texas Red dye (TR) was used with lipid bilayers due to its high stability against photobleaching. The final degree of labeling, one dye molecule per 10 protein molecules, was determined by spectrophotometry.

Crystal Formation on Vesicle Surface. To grow streptavidin crystals on the surface of SOPC/Biotin-X-DHPE vesicles, 80 μ L of the newly electroformed vesicles were added to 420 μ L of protein solution. The protein solution consists of either pure streptavidin or a streptavidin/TR-avidin mixture in 608 mOsm sucrose at an overall concentration of 10–30 μ g/mL. Pure 608 mOsm sucrose solution has a pH of approximately 5; we controlled the pH range of the protein solution from 4 to 7.5 by adding 0.1–2 μ L of either 500 mM Tris, pH 10, or 500 mM MES, pH 3.15. MES and Tris were chosen despite their suboptimal buffering capacity, since they provide far greater stability to the vesicles than all other types of buffers tested. Care was taken to keep the total buffer concentration in the protein solution under 2 mM, as higher ionic concentrations reduce vesicle stability. The vesicles were incubated in the protein solution for at least 3 h at room temperature before observation.

Micromanipulation. We manipulate vesicles with micropipets with an inner diameter between 4 and 10 μ m. To this end, glass capillaries (Hilgenberg, Malsfeld, Germany) with an outer diameter of 1 mm and an inner

(33) Angelova, M. I.; Soléau, F.; Méléard, P.; Faucon, J. F.; Bothorel, P. *Prog. Colloid Polym. Sci.* **1992**, *89*, 127–131.

diameter of 0.5 mm were formed into needles with long tips using a pipet puller (Sutter, San Rafael, CA). The tips were broken with a microforge to form an open and even end with a diameter of the necessary size.³⁴ The inner diameter of the pipets was measured by insertion of gold-coated glass needles that were calibrated by scanning electron microscopy (SEM). The length of the needle inside the pipet was measured with the light microscope; its radius at this point was known from the SEM pictures. With this procedure the inner diameter of the pipets was determined to an accuracy of at least 0.1 μm .

The micropipets were filled with double deionized water by using a Microfil plastic cannula (World Precision Instruments, Berlin, Germany) and inserted into an injection holder (HI-7 Narishige International, London, UK). The holder was placed into a three-axis water hydraulic micromanipulator (MHW-3, Narishige) that was attached to a coarse manipulator (MMN-1, Narishige). The holder is connected to a hydraulic system that allows the application of suction pressure to the pipet.³⁴ Pressures up to 8 kPa were measured with a U tube to an accuracy of 50 Pa.

The micromanipulation chamber was formed by attaching a glass cover slip and 2-mm-thick spacers to a plexiglass block with vacuum grease (Siliconfett medium, Wacker Chemie GmbH, Munich, Germany). To control temperature, the chamber was cooled by circulating thermostated water through channels in the Plexiglas block. The chamber was open on two sides to allow easy access for the micropipet. It was filled with 500 μL of glucose solution with 1 mg/mL bovine serum albumin (BSA) to prevent the vesicles from adhering to glass surfaces. The experiments were performed on the stage of an inverted light microscope (Axiovert 135TV, Carl Zeiss, Jena, Germany) equipped with a LD-Achroplan 40 \times 0.60 Korr lens (Carl Zeiss). For fluorescence microscopy and differential interference contrast (DIC) microscopy, the appropriate optical accessories (filters and Wollaston prisms) recommended by the microscope manufacturer were used. Images were taken with a CCD camera C2400-75I controlled by an Argus 20 image processor (Hamamatsu Photonics, Hamamatsu City, Japan). The latter was connected to the SCSI controller of a PC. Still images were taken by direct transfer of digital data from the image processor to the PC. Movies were acquired by data storage on videotape (Panasonic AG-7350 S-VHS recorder, Panasonic, Matsushita Electric Industrial Corp., Osaka, Japan) and subsequent digitization using a Power Macintosh 8600/250 computer (Apple Computer, Cupertino, CA) equipped with a frame-grabber card LG3 (Scion Corp., Frederick, MD). The programs NIH Image 1.58 VDM and ImageJ (W. Rasband, National Institutes of Health, Bethesda, MD) were used for image processing and measurements.

To determine the elastic area expansion modulus, we followed Kwok and Evans.³⁵ Upon aspiration of a fluid phase lipid vesicle, its membrane is tensed. The mechanical surface tension, T , is given by

$$T = \frac{1}{2} \Delta P \frac{R_p R_0}{R_0 - R_p} \quad (1)$$

where R_p and R_0 denote the radii of the pipet and the vesicle, respectively, and ΔP is the applied aspiration pressure. For uncoated vesicles from phospholipids in the fluid phase, the membrane response shows two different

regimes. At membrane tensions below approximately 0.1 mN/m, membrane bending is probed, i.e., here the reduction of thermally driven undulations is the most important process. The elastic increase of the bare membrane surface dominates at higher tensions,³⁶ producing a linear dependence of the relative area expansion α on the membrane tension.

$$T = T_0 + K\alpha \quad (2)$$

Here, K is the elastic area expansion modulus. The relative area expansion, α , can be calculated with the radii R_p and R_0 and the change of the projection length, ΔL , inside the pipet.³⁶

$$\alpha = \frac{\Delta A}{A_0} \approx \frac{2\pi R_p}{A_0} \left(1 - \frac{R_p}{R_0}\right) \Delta L \quad (3)$$

We measured the relative area expansion, α , for a number of different membrane tensions for each vesicle. The data where reversible, i.e., increasing and decreasing the membrane tension yielded identical results. The actual area expansion moduli were calculated from fits to linear plots of α versus T .

Vesicles were aspirated by pipets with inner diameters between 5 and 6 μm with preset suction pressures between 300 and 3000 Pa for pressure pulse experiments. The time course of aspiration and the subsequent motion of the aspirated part of the vesicle into the pipet were recorded with a time resolution of 25 frames per second.

Membrane Mobility. For a qualitative investigation of the lateral mobility of the membrane components, vesicles were prepared such that they either contained fluorescently labeled lipid (1 mol % NBD-PC from Molecular Probes) or were coated with fluorescently labeled streptavidin (Texas-Red label, see above). These vesicles were observed by using a standard fluorescence microscope (Zeiss Axiovert 200, equipped with a Plan-Neofluar 100 \times /1.3 oil lens, a 100-W mercury arc lamp, and the appropriate filter sets, all supplied by Carl Zeiss, Jena, Germany; an ORCA ER digital CCD camera manufactured by Hamamatsu Photonics, Hamamatsu City, Japan was used for observation). First, an image of the entire vesicle was recorded, the illumination aperture was then closed down and the light intensity was increased by a factor of 12. This resulted in rapid bleaching of the fluorophores within the illuminated area. Subsequent redistribution of the fluorescent molecules was followed with sequential fluorescence micrographs of the entire vesicle at a reduced excitation light intensity.

Confocal Microscopy. The vesicles coated with the streptavidin/TR-avidin mixture were transferred to a viewing cell filled with 618 mOsm glucose solution containing 1 mg/mL BSA. The lower density of surrounding glucose solution causes the sucrose-filled vesicles to sink to the bottom of the cell and remain still during observation.

The confocal laser scanning microscope consists of a scanning unit (Noran, Middleton, WI) attached to a Zeiss Axiovert 100 TV (Zeiss, Germany). The vesicles were scanned with a laser passing through a 568/590LP excitation/emission filter set and viewed with an LD-Achroplan 40 \times 0.60 Korr lens (Carl Zeiss). To prevent superposition of images from opposite sides of the vesicle, image slices of only the upper half of the vesicles were taken at 0.5–1- μm intervals and a three-dimensional reconstruction was created by using the Intervision

(34) Evans, E. A. *Methods Enzymol.* **1989**, 173, 3–35.

(35) Kwok, R.; Evans, E. *Biophys. J.* **1981**, 35, 637–652.

(36) Evans, E.; Rawicz, W. *Phys. Rev. Lett.* **1990**, 64, 2094–2097.

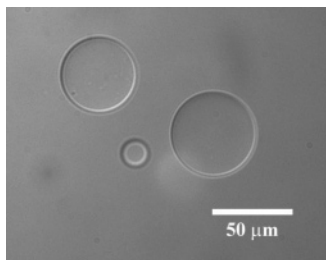


Figure 1. DIC Microscopy image of bare SOPC/Biotin-X-DHPE vesicles.

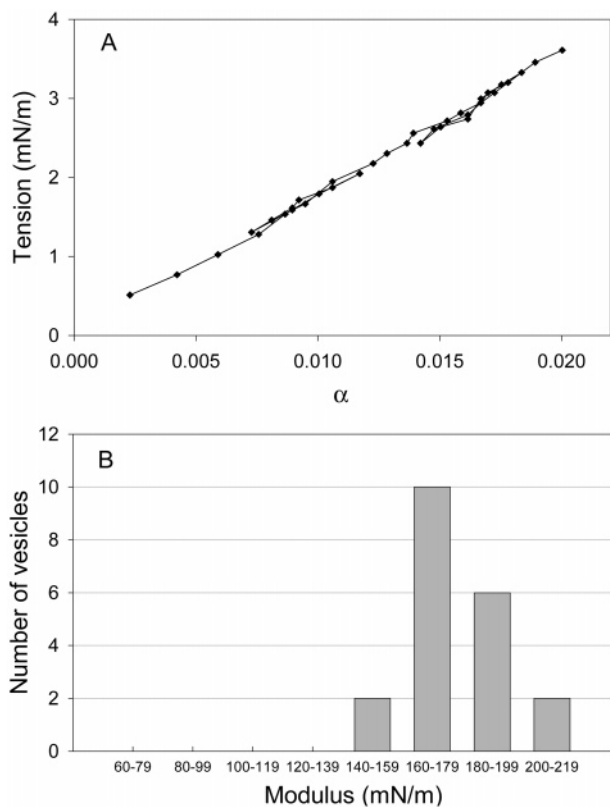


Figure 2. (A) Typical membrane tension vs fractional area expansion (α) data for bare SOPC/Biotin-X-DHPE vesicles. (B) Distribution of area expansion moduli. The average value is 177 mN/m with a standard deviation of 15 mN/m ($n = 20$).

software package provided by Noran on a Silicon Graphics Indy II computer (SGI Inc., Mountain View, CA).

Results

Bare SOPC/Biotin-X-DHPE Vesicles. The electroformation method described above yields numerous stable, round vesicles between 10 and 60 μm as shown in Figure 1. At higher external glucose concentrations, the vesicles are deflated and lose their spherical shape due to the large excess area on the surface.³⁷ Thermal fluctuations on the membrane can clearly be seen when the vesicles are viewed under these conditions.

We examined the area expansion moduli of these vesicles. The projection changes rapidly and smoothly in response to the applied tension as shown in Figure 2A. The points are connected to show the responses to sequential changes in the pipet suction pressure. The superimposition of the increasing and decreasing suction pressure data onto a single line indicates the vesicle's elastic response to area dilation. The average area

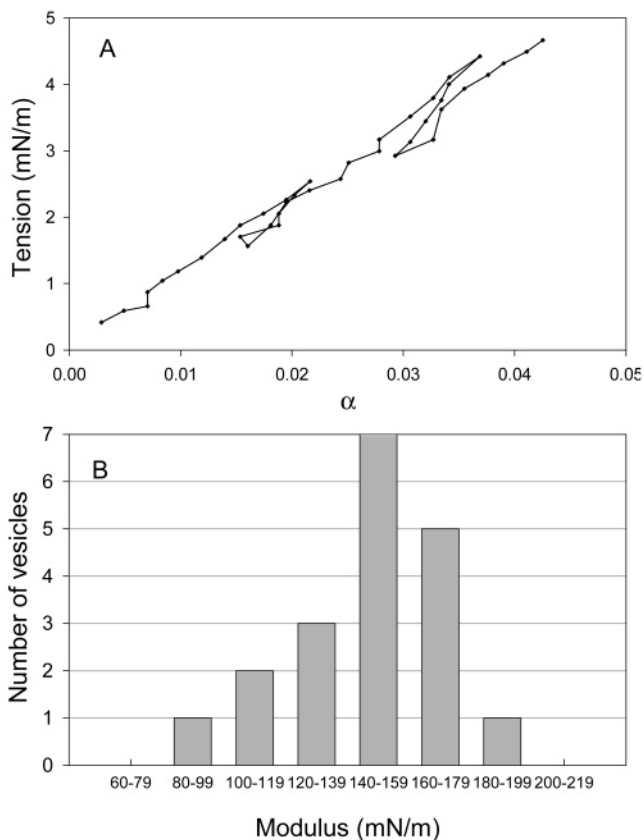


Figure 3. (A) Typical membrane tension vs fractional area expansion (α) measurement for avidin-coated vesicles. (B) Distribution of area expansion moduli. The average value is 146 mN/m with a standard deviation of 27 mN/m ($n = 19$).

expansion modulus of 177 ± 15 mN/m ($n = 20$) was in close agreement to literature values for pure SOPC vesicles of approximately 180 mN/m.^{36,38,39}

Figure 2B shows the relatively narrow distribution of the area expansion moduli of bare vesicles. The distribution of moduli is plotted on the same scale as those obtained for avidin and streptavidin-coated vesicles presented below. The bare vesicles rupture very rapidly; the entire rupturing process generally takes less than one second and can be characterized by the membrane vanishing into the pipet.

Avidin-Coated SOPC/Biotin-X-DHPE Vesicles. After incubation with avidin, the vesicles were still smooth, spherical, and devoid of creases and folds; however, membrane undulations were no longer visible even when the vesicles were placed in a significantly higher osmolarity glucose solution (839 mOsm). This implies a significant increase in membrane bending stiffness. Due to the high isoelectric point (pI) of avidin (pI ~ 10), the avidin-coated vesicles adhered to the glass surfaces. The effect was greatly reduced, though not completely eliminated, through the addition of higher concentrations of BSA (2 mg/mL) into the solution. Micropipet aspiration of vesicles with fluorescently labeled avidin clearly showed the presence of protein on the aspirated portion of the membrane, indicating that the membrane and protein layer is aspirated together. Their area expansion moduli are similar to those of bare vesicles, as shown in a typical data set (Figure 3A). The average area expansion modulus of avidin-coated vesicles is 146 ± 27 mN/m ($n = 19$). The

(37) Lipowsky, R. *Nature* **1991**, *349*, 475–481.

(38) Hianik, T.; Paschnick, V. I. *Bilayer Lipid Membranes: Structure and Mechanical Properties*; Kluwer Academic Publishers: Boston, 1995.
(39) Needham, D.; Nunn, R. S. *Biophys. J.* **1990**, *58*, 997–1009.

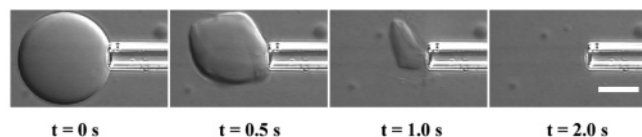


Figure 4. DIC image sequence of a typical rupturing process of avidin-coated vesicles, showing a slow “deflation” behavior. Scale bar represents 10 μm .

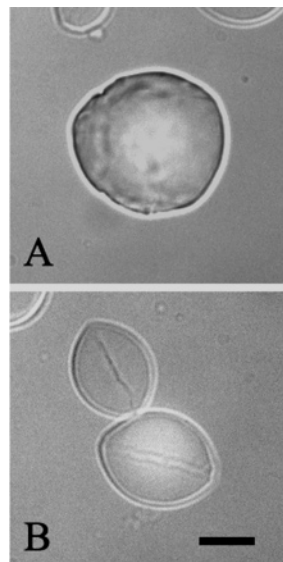


Figure 5. DIC microscopy images of two typical morphologies of streptavidin-coated vesicles. (A) Spherical vesicles with rough surfaces. (B) Football-shaped ellipsoids have smoother surfaces with characteristic ridges parallel to the major axis. Scale bar is 20 μm .

comparatively large scatter of the data is caused by residual adhesion of the membrane to the pipet.

Despite their similarity to bare vesicles, avidin-coated vesicles show a dramatically different rupturing behavior. Instead of the rapid instantaneous rupture normally seen, the coated vesicles break with a much slower deflation process (Figure 4). Although the actual deflation time depends on the applied suction pressure and vesicle size, typical time scales for the rupturing process are on the order of seconds. The slow deflation and the lack of visible rigid edges and creases are indicative of the presence of a protein shell, which is most likely fluid.

Streptavidin-Coated SOPC/Biotin-X-DHPE Vesicles. When the vesicles were incubated with pure streptavidin, they were no longer smooth and spherical. Instead, the vesicles were more rigid with numerous creases and facets on the surface, indicative of the presence of a polycrystalline shell. Thermal undulations were no longer seen. Unlike avidin-coated vesicles, the streptavidin-coated vesicles remained unperturbed by strong nudges with the micropipet tip. In general, we observed two typical vesicle morphologies shown in Figure 5.

The two morphologies coexist within the same sample, with an increasing fraction of prolate ellipsoids at higher pH.²⁷ Both morphologies have similar elastic behavior and properties.

To verify that streptavidin crystals are present on the surface of these giant vesicles, we performed laser scanning confocal microscopy studies on vesicles coated with a mixture of streptavidin and TR-avidin. Figure 6 shows images of vesicles coated with approximately a 1:1 mixture of streptavidin and TR-avidin. Avidin was included to dilute the streptavidin at the surface, allowing uninhibited growth of larger crystalline domains. The streptavidin

crystals can be seen in fluorescence microscopy because the labeled avidin is excluded from the crystals.

Unlike the vesicles in Figure 5, the vesicles in Figure 6 remained relatively smooth and round due to the low crystallite density on the surface in the presence of avidin. The crystalline area increases with the amount of streptavidin on the surface, and covers the entire vesicle surface when 100% streptavidin is used.

Streptavidin vesicles also rupture by slow deflation with a time scale on the order of seconds. One difference from the case of avidin-coated vesicles is the presence of sharp ridges during the crumpling process as shown in Figure 7.

Another property unique to streptavidin-coated vesicles is permanent deformation. Figure 8 shows an image sequence of a streptavidin-coated vesicle being aspirated into a micropipet and quickly released. The deformation did not recover within the observation time of 1.5 h, characteristic of a plastic behavior.

Streptavidin-coated vesicles also show shape changes when aspirated by using a micropipet. The vesicle gradually changes from its rough spherical shape into a smoother form (Figure 9).

A representative vesicle response to a stepwise increase in suction pressure is shown in Figure 10. At tensions up to approximately 2 mN/m, the vesicle is permanently deformed, and the projections do not retract when suction pressure is reduced. Friction forces between the vesicle and the glass wall of the pipet were not the cause of this behavior, as the vesicle and its permanently deformed projection easily slides out of the pipet when the suction pressure is removed as shown in Figure 8. In addition, the membrane response in this low-pressure regime is almost instantaneous. When tensions above approximately 2 mN/m are applied, additional deformations are no longer permanent. Instead, the vesicle projection shows a slower exponential viscoelastic response, and the projection length increases proportionally to the suction pressure (Figure 10). It is worth noting that all the streptavidin-coated vesicles studied using micropipet aspiration exhibited the permanent deformation-viscoelastic transition regardless of vesicle morphology. At these tension values, the applied strain likely involves the direct area dilation of the vesicles. Despite the polycrystalline nature of the composite protein-lipid membrane, which likely imposes an anisotropic strain to the vesicle, the membrane response to stepwise increase in tension is linear.

Using an analysis similar to that of Discher et al. on cross-linked polymer vesicles,⁴⁰ the slope of plots of nominal tension vs dimensionless projection length $x = L/R_p$ can be related to the elastic area expansion moduli,⁴¹ resulting in the expression $K \approx 32d\tau/dx$ for R_0/R_p values of 2.5–4.1. This yields $K = 68 \pm 27$ mN/m. In general, once deformed past 2 mN/m, the streptavidin-coated vesicles showed much less resistance against area dilation than either bare or avidin-coated vesicles. Despite the rigid appearance, the vesicles rupture at tensions of 4.9 ± 1.3 mN/m ($n=15$), within error to that obtained from uncoated pure SOPC vesicles (5.7 ± 0.2 mN/m).³⁹ Not surprisingly, the distribution of the values is broad due to large variations in the structure of the polycrystalline shell.

To study the vesicle response to sudden changes in suction pressure, a series of alternating pressure pulses

(40) Discher, B. M.; Bermudez, H.; Hammer, D. A.; Discher, D. E. *J. Phys. Chem. B* **2002**, *106*, 2848–2854.

(41) Evans, E. A.; Skalak, R. *Mechanics and Thermodynamics of Biomembranes*; CRC Press: Boca Raton, 1980.

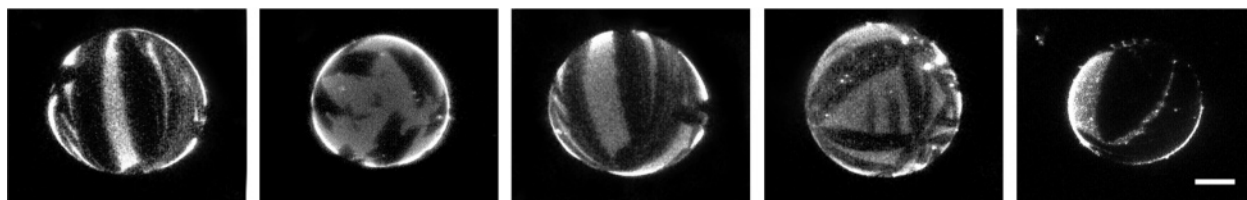


Figure 6. Three-dimensional reconstructed confocal microscopy images of giant vesicles containing biotin-functionalized phospholipid and incubated with 1:1 streptavidin/Texas-Red avidin mixtures. The crystals of unlabeled streptavidin appear as black domains surrounded by fluorescent noncrystallizable avidin. Five different vesicles are shown to illustrate the various crystal domains. Scale bar represents 10 μm .

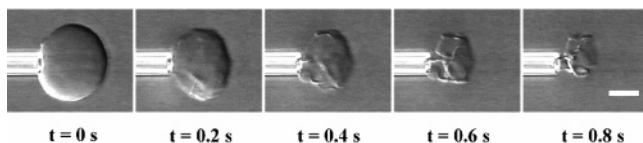


Figure 7. Video image sequence of the rupturing process of streptavidin-coated vesicles showing a slow crumpling behavior and the presence of sharp edges on the surface. Scale bar represents 10 μm .

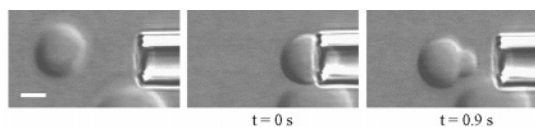


Figure 8. Video image sequence of a streptavidin-coated vesicle being partially aspirated into a micropipet and quickly released. The persistent deformation after release indicates plastic deformation. Scale bar is 5 μm .

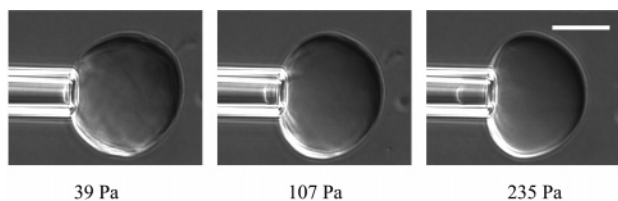


Figure 9. Shape changes of a streptavidin-coated vesicle upon aspiration. The numbers indicate the suction pressure inside the micropipet. At higher suction pressures, the membranes shows wrinkles near the pipet, and the vesicle takes on a nonspherical shape. The shape is maintained until rupture at greater than 3000 Pa. Scale bar is 20 μm .

and relaxation periods were applied to the vesicles. A representative profile of the vesicle projection length vs pressure is shown in Figure 11.

In general, when a pressure pulse under 1000 Pa is applied, the response is almost instantaneous. The vesicle projection remains after the suction pressure is reduced, and no significant increase in length occurs if a subsequent pressure pulse of the same magnitude is applied. When a suction pressure above the threshold (approximately 1000 Pa) is applied, the vesicle responds with a slower exponential viscoelastic behavior. When the pressure is subsequently reduced, the vesicle projection only partially recovers, and usually a slight increase in the permanent projection length is observed.

We also performed mobility tests to qualitatively study the fluidity of the lipid bilayer compared to that of the outer streptavidin shell. The test was done by selectively incorporating the corresponding layer with a fluorescent dye, which was then bleached and the fluorescence recovery was monitored. Figure 12 shows the fluorescence recovery of a bleached area on a streptavidin-coated vesicle in which fluorescent NBD-PC lipid was incorporated into the lipid bilayer.

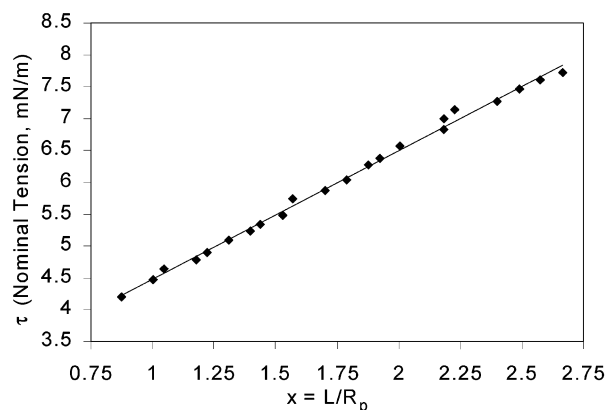


Figure 10. Typical plot of nominal tension τ vs dimensionless projection length $x = L/R_p$ for streptavidin-coated vesicles. The vesicle projection length increases linearly with the applied suction pressure.

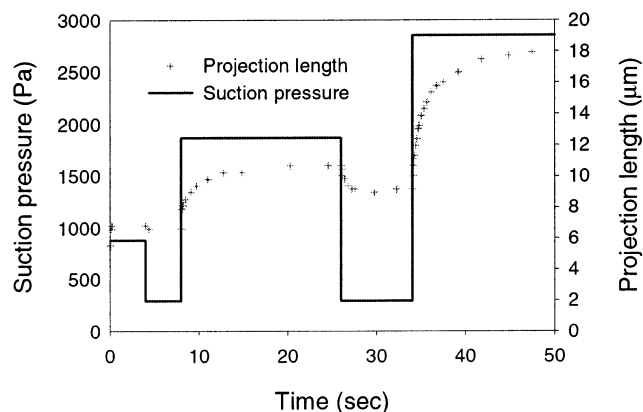


Figure 11. Representative response profile of streptavidin-coated vesicles to alternating pressure pulse and relaxation periods. The + symbols represent the vesicle projection lengths, while the solid line marks the applied suction pressures being applied. The diameters of the vesicle and the pipet in this particular experiment are 29.5 and 6.6 μm , respectively.

The lipid fluorescence in the photobleached region recovers fairly rapidly. The recovery rate is comparable to that of bare vesicles (bare vesicles recover approximately twice as fast, data not shown). When the streptavidin layer is selectively labeled and photobleached, on the other hand, the fluorescence did not recover over a period of 153 s, indicating the solidlike nature of the crystalline shell (Figure 13).

By selectively photobleaching the two layers, we observed that despite the strong coupling between the streptavidin crystals and the biotin-functionalized lipid bilayer, the lipid bilayer remains fluid while the streptavidin layer is immobilized as a polycrystalline shell.

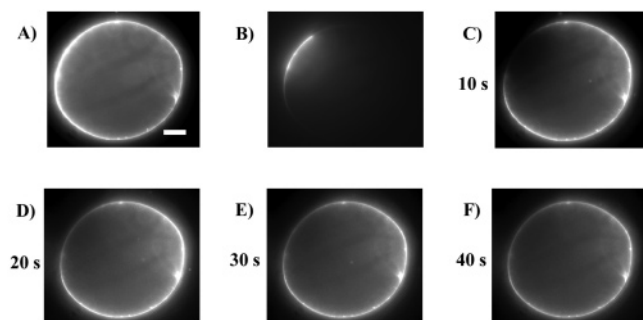


Figure 12. Fluorescence recovery of a photobleached region on a streptavidin-coated vesicle where fluorescent NBD-PC phospholipid molecules were incorporated in the lipid bilayer. (A) The initial streptavidin-coated vesicle. (B) Photobleaching of the upper left corner of the vesicle. (C–F) Series of images showing the fluorescence recovery of the lipid layer. The bleached edge on the upper left side of the vesicle was clearly visible in less than 60 s. Scale bar is 10 μm .

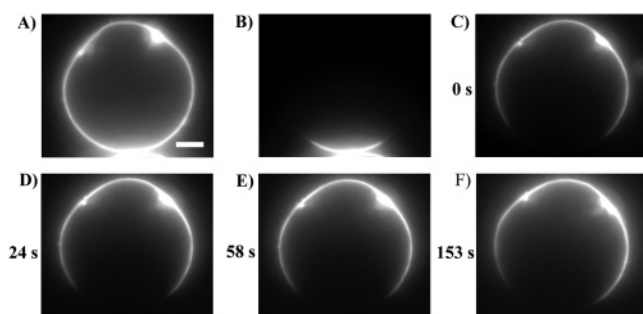


Figure 13. Fluorescence recovery of a photobleached region on a streptavidin-coated vesicle where the streptavidin molecules were fluorescently labeled with Texas-Red. (A) The initial streptavidin-coated vesicle. (B) Photobleaching the bottom area on the vesicle. (C–F) Sequential images following the photobleaching. The bleached vesicle edge was no longer visible. Scale bar is 5 μm .

Discussion and Analysis

When the bare vesicles were incubated with either avidin or streptavidin, the protein layer suppressed the thermal undulations and made the membranes more rigid. The tightly bound protein layer reduces lipid mobility and produces a viscoelastic response to expansion. In conjunction with the relatively large size of the protein molecules, protein–protein and protein–lipid interactions contribute to the reduction of membrane flexibility.

Avidin-coated giant bilayer vesicles have been studied by Noppl-Simon and Needham in the context of vesicle adhesion and cross-bridge formation.⁴² The effect of avidin on the elastic moduli of giant vesicles has not been reported. Avidin molecules on the vesicle surface behave as a two-dimensional liquid, and the lateral interactions between them are weaker than those in streptavidin. Mean-field analysis indicates a crystallization energy of approximately $10k_{\text{B}}T$, where k_{B} is the Boltzmann constant and T is the absolute temperature.⁴³ Although the energetic difference is not large, its effect on the vesicle properties is quite pronounced. The avidin-coated vesicles show characteristics similar to those of bare vesicles, such as the spherical shape and elastic recovery after deformation, and similar values for the area expansion modulus. The data for the area expansion modulus is more widely

scattered than that for bare vesicles due to the noticeable affinity of the avidin-coated vesicles to the glass pipet, as shown in Figure 3B. The slow rupturing of the avidin-coated vesicles indicates an increased dissipation caused by the avidin layer on the surface.

Streptavidin-coated vesicles show dramatically different properties from those of bare and avidin-coated vesicles. It is obvious from Figure 6 that streptavidin crystallites are present on the surface, and are responsible for the unique behavior seen. As Figure 5 shows, two typical vesicle morphologies are observed. Confocal microscopy images show that streptavidin crystallites on the vesicle surface tend to exhibit strong shape anisotropy due to a preferential growth direction. This effect is more pronounced at higher pH values.²⁷ Such shape anisotropy in conjunction with parallel growth directions of multiple crystallites to minimize the overall bending energy can lead to the distortion of the vesicles along one axis.

Perhaps the most distinct characteristic of the streptavidin-coated vesicles is the rapid permanent deformation followed by slow viscoelastic relaxation. Under the specified experimental conditions, the transition point between these two responses occurs at approximately 1000 Pa of suction pressure or at approximately 2 mN/m of tension. In most cases, even a small suction pressure of 300 Pa is sufficient to form a permanent projection.

Permanent (plastic) deformation behavior has been reported in biological membranes such as red blood cells⁴⁴ and, more recently, in polyelectrolyte microcapsules.⁴⁵ Although streptavidin-coated vesicles are significantly simpler in composition, they are also capable of producing plastic deformation.

The first indication of the underlying mechanism can be found in the apparent area expansion modulus of streptavidin-coated vesicles. The estimated values are significantly lower than those obtained from bare or avidin-coated vesicles.

According to recent studies, the value for the Young's modulus for similar protein crystals such as lysozyme and ribonuclease fall in the range 0.5–17.5 GPa.⁴⁶ Based on these values, the analogous two-dimensional values of the area expansion modulus can be calculated by⁴¹

$$K = \frac{hE}{2(1-\nu)} \quad (4)$$

where h is the shell thickness, E is the Young's modulus, and ν is Poisson's ratio. If we assume a value of 5 nm for the shell thickness and 0.5 for Poisson's ratio of an incompressible material, the approximate values of K range between 2.5×10^3 and 8.75×10^4 mN/m. These values are at least an order of magnitude greater than those obtained from streptavidin-coated vesicles and are the first indications that the two-dimensional streptavidin crystallites remained relatively undeformed on the vesicle surface throughout the membrane deformation.

The presence of permanent deformation at very low suction pressures along with the absence of a detectable linear elastic regime and yield point suggest that the observed behavior is different from plastic deformations typically observed in other materials. From linear elasticity theory, we can estimate the material strain in a 5-nm-thick elastic plate aspirated into a 4- μm micropipet to

(44) Evans, E. A.; LaCelle, P. L. *Blood* **1975**, *45*, 29.

(45) Bäuml, H.; Artmann, G.; Voigt, A.; Mitlöhner, R.; Neu, B.; Kieseewetter, H. *J. Microencapsul.* **2000**, *17*, 651–655.

(46) Caylor, C. L.; Speziale, S.; Kriminski, S.; Duffy, T.; Zha, C.-S.; Thorne, R. E. *J. Crystal Growth* **2001**, *232*, 498–501.

(42) Noppl-Simon, D. A.; Needham, D. *Biophys. J.* **1996**, *70*, 1391–1401.

(43) Coussaert, T.; Völkel, A. R.; Noolandi, J.; Gast, A. P. *Biophys. J.* **2001**, *80*, 2004–2010.

protrude $0.5\ \mu\text{m}$ of less than 0.25%.⁴⁷ In our experiments we observe plastic behavior at those small deformations. This estimate implies that a streptavidin-coated membrane has an exceptionally low yield point for plastic flow.

Experimental evidence suggests that the streptavidin-coated vesicle can be represented by a two-layer spherical shell model. The outer layer is a rigid polycrystalline shell attached to the underlying lipid bilayer by biotin-conjugated phospholipid anchors. At the experimental pH of 5.0, the charge density of streptavidin on the biotin-binding face is essentially zero,⁴⁸ thus the net electrostatic interactions with the neutral SOPC lipids should be minimal. Streptavidin is also known to have negligible nonspecific binding to neutral phospholipids, as evident from ellipsometric measurements⁴⁹ and purely repulsive force-distance profiles between streptavidin and bare neutral phospholipid monolayers obtained by using the surface force apparatus.⁵⁰ As the crystal domains grow on the vesicle surface, small amounts of noncrystalline streptavidin are concentrated in regions between crystalline domains and prevent further crystallization. When the vesicles were placed in the manipulation chamber filled with a hyperosmotic glucose solution, osmotic shrinkage occurs; however, due to the tightly packed crystallites, the vesicles could not take on the diverse shapes normally observed under such conditions.^{37,51} This results in corrugations in the underlying lipid bilayer at the noncrystalline areas between crystalline domains (Figure 14A). DIC microscopy images of streptavidin vesicles support this model, as numerous creases and ridges are visible from the surface of vesicles in this state.

When a small amount of suction is applied to the vesicle using a micropipet, the corrugations are merely straightened out (Figure 14A-B). Since the deformation involves simply the smoothing of the corrugations by aspirating parts of the excess bilayer area into the pipet without significant area dilation, the projection remains rigid and permanent. Aspiration of Texas-Red streptavidin-coated vesicles confirms that both the protein and the excess lipid bilayer are aspirated into the pipet. Since the major corrugations occur between grain boundaries, viscous dissipation due to lipid flow is negligible in this region, and the vesicles respond rapidly in this regime. After release of the suction pressure the lipid bilayer exerts negligible force on the polycrystalline shell.

As the suction pressure increases, this process continues until the major corrugations have been extended (Figure 14C). At the transition point, further aspiration of the vesicle results in area expansion of the underlying bilayer membrane, and the elastic properties of the bilayer dominate. In addition to the immobilized biotin-X DHPE pillars hindering movement of other lipid molecules, lipid flow against a rigid surface produces hydrodynamic friction.⁵² The two effects create significant dissipation in the bilayer, resulting in the observed exponential viscoelastic response of the membrane. The membrane area shrinks again following the release of aspiration pressure. Therefore the lipid bilayer exerts a restoring force on the

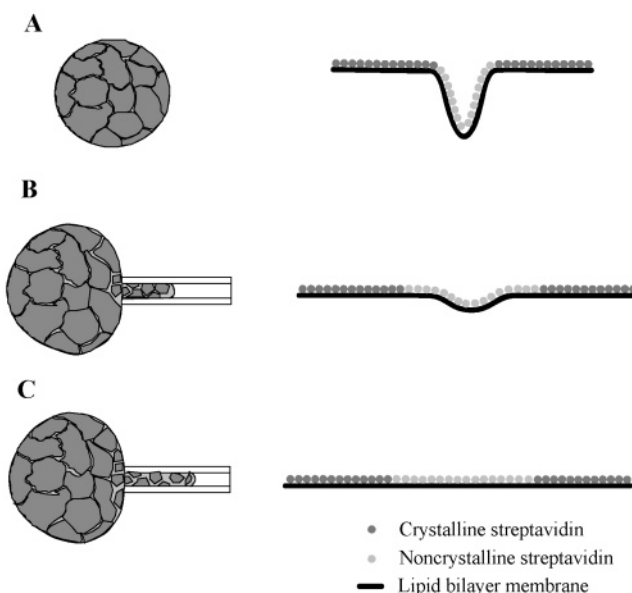


Figure 14. Schematic drawing of streptavidin crystals on the surface of a bilayer vesicle subjected to micropipet aspiration (not drawn to scale). (A) Osmotic shrinkage along with the high rigidity of streptavidin crystals produces corrugations in the lipid bilayer. Micropipet aspiration of the vesicles in this state stretches out the corrugations at constant bilayer surface area. (B) The process continues until major corrugations are stretched, after which the bilayer membrane tension begins to increase. (C) Further aspiration of the vesicle leads to surface area expansion of the lipid bilayer, and the elastic properties of the bilayer membrane dominate. The polycrystalline shell remains relatively intact throughout most of the vesicle surface.

polycrystalline shell, which is responsible for the observed elastic behavior in the high-tension regime.

The fate of the streptavidin crystallites during these processes can be deduced from the equilibrium shape of the aspirated vesicle. Figure 9 shows that the vesicle remains nonspherical during most of the aspiration process due to the persistence of large crystalline domains at the surface of the vesicle. Thus, with exception of areas in the vicinity of the pipet tip, the crystal network should remain relatively intact, and area dilation of the lipid bilayer should occur without significant perturbation to the outer protein layer.

To account for the apparently low area expansion moduli of streptavidin-coated vesicles relative to those of bare or avidin-coated vesicles, the two-layer composite membrane can be thought of as a Hookean element with two elastic springs in series. The first spring represents the elastic response of the lipid bilayer, while the second spring results from the protein crystals. Streptavidin crystals exist as flat rigid patches on the vesicle surface and do not easily conform to the curvature of the bilayer surface. The vesicle thus appears to have many edges and facets. At increasing tensions, the facets are progressively smoothed out as the surface area of the membrane increases. Connecting the two elements in series results in a combined spring constant that is smaller than that of the individual elements. Since the extent of total area dilation depends also on the nature of the polycrystalline structure, inhomogeneity in the crystalline shell causes a greater variation in the values of the measured moduli.

As we have shown, streptavidin-coated vesicles show combined properties of both the streptavidin crystals and the fluid lipid bilayer to yield thin, rigid, yet viscoelastic composite membrane. In contrast to their rigid appearance, the existence of a polycrystalline shell does not

(47) Landau, L. D.; Lifschitz, E. M. *Theory of Elasticity*; Pergamon Press: London, 1959; Vol. 7.

(48) Sivasankar, S.; Subramaniam, S.; Leckband, D. *Proc. Natl. Acad. Sci. U.S.A.* **1998**, *95*, 12 961–12 966.

(49) Reiter, R.; Motschmann, H.; Knoll, W. *Langmuir* **1993**, *9*, 2430–2435.

(50) Sheth, S. R.; Leckband, D. *Proc. Natl. Acad. Sci. U.S.A.* **1997**, *94*, 8399–8404.

(51) Dobreiner, H. G.; Kas, J.; Noppl, D.; Sprenger, I.; Sackmann, E. *Biophys. J.* **1993**, *65*, 1396–1403.

(52) Merkel, R.; Sackmann, E.; Evans, E. *J. Phys. (Paris)* **1989**, *50*, 1535–1555.

increase the toughness of the vesicles. The toughness, or cohesive energy density, can be estimated from the integral of the tension with respect to areal strain up to the point of rupture.^{53,54} Streptavidin-coated vesicles have a toughness of $0.11 \pm 0.05 \text{ mJ/m}^2$ ($n=15$), within error of the value obtained from bare SOPC vesicles.³⁹ Thus under high-tension, streptavidin-coated vesicles show elastic properties of the underlying lipid bilayer, while retaining the rigid characteristics of a polycrystalline shell. Certain characteristics including the rigid appearance, vesicle shape transition during aspiration, and the formation of wrinkles are strikingly similar to those found in cross-linked block copolymer vesicles;⁴⁰ however, they do not see the more complex behavior seen here such as plastic deformation and viscoelasticity due to their simpler membrane composition.

The experimental data presented above clearly show that the extent of protein–lipid interaction influences the properties of the composite membrane. In the case of most bacterial surface layers, the s-layer proteins are known to interact with the lipid bilayer via strong electrostatic interactions. Such interactions would surely involve the majority of lipid molecules under the protein layer. The situation is different with streptavidin-coated vesicles, where strong electrostatic interactions between neutral SOPC phospholipids and streptavidin molecules were not present, and the majority of interactions occur by the biotin–streptavidin ligand–receptor interaction.⁴⁹ Each streptavidin molecule is pinned to the bilayer by at most two biotin-functionalized phospholipids, while the rest of the lipid molecules remain relatively independent of the

protein layer. Despite this minimal interaction with the lipid layer, streptavidin-coated vesicles show significant morphological and mechanical changes with protein ordering.

Conclusion

Through the use of micropipet manipulation and microscopy, we studied the effects of a monomolecular layer of avidin or streptavidin on giant lipid bilayer vesicles. Binding of noncrystallizable avidin increased the bilayer bending rigidity and greatly suppressed thermal undulations. The elastic response to dilation of the vesicles was not significantly altered over that of bare vesicles. When the vesicles were coated with streptavidin, more complex behavior resulted. In addition to the dramatic reduction in thermal undulations seen with avidin-coated vesicles, the streptavidin crystallizes into a two-dimensional polycrystalline shell. The crystal morphology along with the high bending rigidity of the crystallites transformed the vesicles into roughened spheres and prolate ellipsoids. The composite protein–lipid membrane combines the solid characteristics of two-dimensional crystals with the fluid elastic behavior of lipid bilayers to yield a thin, rigid, yet viscoelastic structure. The nature of the protein–lipid and protein–protein interactions plays a key role in determining the overall properties of the composite membrane.

Acknowledgment. This work was supported by NASA Grant NAG3–2398 and the grant Me1458/3 by the Deutsche Forschungsgemeinschaft (DFG).

(53) Callister, W. D. *Materials Science and Engineering: An Introduction*; Anderson, W., Ed.; John Wiley & Sons: New York, 2000.

(54) Discher, B. M.; Won, Y.-Y.; Ege, D. S.; Lee, J. C.-M.; Bates, F. S.; Discher, D. E.; Hammer, D. A. *Science* **1999**, *284*, 1143–1146.